SCIENCE CHINA
Chemistry

• ARTICLES •

March 2016 Vol.59 No.3: 293–302
doi: 10.1007/s11426-015-5477-8

Gelation capability of cysteine-modified cyclo(*L*-Lys-*L*-Lys)s dominated by Fmoc and Trt protecting groups

Huimin Geng, Qianying Zong, Jie You, Lin Ye, Aiying Zhang, Ziqiang Shao & Zengguo Feng*

School of Materials Science and Engineering, Beijing Institute of Technology, Beijing 100081, China

Received May 18, 2015; accepted June 18, 2015; published online October 13, 2015

A series of symmetrical peptidomimetics (**3**–**8**) based on cysteine-modified cyclo(*L*-Lys-*L*-Lys)s were synthesized, and their gelation capability in organic solvents was dominated by fluorenylmethyloxycarbonyl (Fmoc) and triphenylmethyl (Trt) protecting groups and the exchange of thiol-to-disulfide as well. The peptidomimetics holding Trt (**3** and **4**) showed no gel performance, while the Fmoc groups promoted **5** and **6** to give rise to thermo-reversible organogels in a number of organic solvents. The self-assembled fibrillar networks were distinctly evidenced in the organogels by transmission electron microscopy (TEM) and scanning electron microscopy (SEM) observations. Fourier transform infrared spectroscopy (FT-IR) and fluorescence analyses revealed that the hydrogen bonding and π-π stacking play as major driving forces for the self-assembly of these organogelators. A β-turn secondary structure was deduced for the organogel of **6** by virtue of X-ray diffraction, FT-IR and circular dichroism (CD) measurements, and an interdigitated bilayer structure was also presented.

organogel, cyclic dipeptide, self-assembly, cysteine, β-turn

Citation: Geng HM, Zong QY, You J, Ye L, Zhang AY, Shao ZQ, Feng ZG. Gelation capability of cysteine-modified cyclo(*L*-Lys-*L*-Lys)s dominated by Fmoc and Trt protecting groups. *Sci China Chem*, 2016, 59: 293−302, doi: 10.1007/s11426-015-5477-8

1 Introduction

Although low-molecular-weight gelators (LMWGs) possess in general a molecular weight of less than 2000 Da, they are capable of absorbing a large amount of organic solvents or water to create physical organo- and hydrogels in which the molecules are self-assembled into a fixed 3D network of fibers, solely held together by non-covalent interactions [1–3]. Despite the structural diversity, a common theme for LMWGs is that the inherent non-covalent interactions, such as van der Waals interactions, π-π stacking, hydrogen bonding, and electrostatic interactions, drive them to form the self-assembled fibrillar 3D network. As a consequence, most of these gels can respond to external stimuli, e.g. temperature, pH, light, shear and ultrasound with the great potential to be used as solid-like smart materials [3–5].

Amongst the LMWGs, peptidic gelators have attracted tremendous attention in recent years [6,7]. For instance, Zhang *et al*. [7] first discovered that peptides with alternating hydrophobic and hydrophilic amino acid sequences can spontaneously self-assemble into hydrogels used as tissue-engineering and regenerative medical scaffolds. Since then, peptide hydrogels have been witnessed as a fantastic platform that makes them ideal candidates for emerging biomaterial applications due to their nontoxic, easy to use and biodegradable properties [8,9]. At the same time, they have also gained recognition employed for stimuli-responsive materials, sensors, electronic materials and so on [2]. A dipeptide gel-based sensor via a thiol-to-disulfide oxidation of *L*-cysteine derivative could be uniquely used to detect

*Corresponding author (email: sainfeng@bit.edu.cn)

triacetone triperoxide explosive visually without any instrumentation [9]. Interestingly, Fmoc-tripeptides with inverse sequence of Fmoc-VLK(Boc) and Fmoc-K(Boc)LV led to substantial differences in self-assembled secondary structures of well-defined β-sheets and unoriented self-assemblies in hydrogels [10]. In recent articles, Ulijn *et al.* [11,12] had demonstrated a computational design-oriented approach by screening all 8000 possible tripeptides and provided a set of designing rules for self-assembling sequences of peptide-based gelators. Therefore, these short peptides with the simple synthesis, intriguing physical properties and inherent ability to adopt ordered secondary structures enable to gain access to a vast range of well-ordered assemblies at the nanoscale for smart material applications [13].

In particular, as the smallest cyclic peptide molecule, 2,5-diketopiperazine (2,5-DKP) or cyclic dipeptide and its derivatives are often prepared by the condensation of two corresponding α-amino acids [14,15]. The formation of sequential intermolecular hydrogen bonds between N–H and C=O in 2,5-DKPs enables the growth of molecular assemblies [16]. A family of 2,5-DKPs with 32 different structures consisting of diverse amino acids and a branched alkyl group exhibited remarkable gelation abilities by hydrogen-bonded molecular ladders [17]. A bifunctional diketopiperazine containing *L*-aspartic acid induced a reverse turn of the growing peptide chain and its oligomer adopted a β-bend ribbon conformation starting from four units involving 10-membered hydrogen-bonded rings [18]. Furthermore, 2,5-DKP moieties frequently occurred in nature with a specific biological activity and have potential therapeutic applications [16]. Clearly the outstanding structural stability, preferred intermolecular hydrogen bonding interaction, good biological compatibility and molecular recognition ability make these cyclic dipeptides ideal LMWGs. The thixotropic behavior of hydrogel formed from cyclo-(*L*-*O*-hydroxyhexylaspartyl-*L*-phenylalanyl) enabled to be repeated many times [19]. The organogels formed by cyclo(Gly-*L*-Lys) derivatives were employed to physically entrap dye and drug molecules, while the hydrogels were candidate for drug delivery systems and thermo-responsive smart materials [14]. Cyclo(*L*-Tyr-*L*-Lys) was shown to have antinociceptive activity [20]. Feng *et al.* [4] found serendipitously that this cyclic dipeptide can not only yield strong organogels in polar solvents, such as dimethyl sulfoxide (DMSO), (*N*,*N*-dimethylformamide) (DMF) and dimethylacetamide (DMAC), but also form hydrogel via ultrasound. After *N*-acylated with *D*-(+)-gluconic acid, a shear-triggered hydrogel with thixotropic nature was also generated by applying shear force on its metastable supersaturated solution [21]. Meanwhile, fumaryl-modified cyclo(*L*-Lys-*L*-Lys) was reported a safe delivery vehicle for insulin administration via inhalation [22,23]. However, as far as cyclo(*L*-Lys-*L*-Lys) (**1**) is concerned as shown in Scheme 1, it displays no gelation ability due to its cationic characteristic and high solubility in water and most organic solvents [22]. Although **1** holds a 2,5-DKP unit, the structural modification is evidently necessitated to converse it into organo- and hydrogelatos. After the modification, the cyclo(*L*-Lys-*L*-Lys) derivatives should be imparted a strong ability to gel a number of organic solvents and water with the potential to be used in a wide range of applications including scaffolds for tissue engineering and regenerative medicine, carriers for drug controlled release, biosensors and catalysts, absorbents for waste water purification, etc. [22,23]. Herein, a series of symmetrical pepetidomimetics (**3–8**) were synthesized through the modification of cyclo-(*L*-Lys-*L*-Lys) using cysteine in which both noncyclic peptidomemitic **5** and bicyclic peptidomemitic **6** enabled to gelate most organic solvents in this study. Their gelation behaviors were dominated by Fmoc and Trt protecting groups as well as the thiol-to-disulfide oxidation.

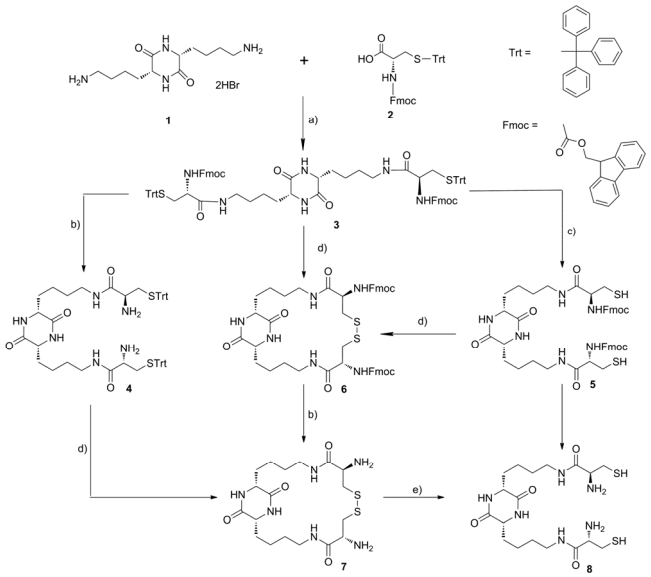

Scheme 1 Synthetic route of symmetrical peptidomimetics derived from cysteine-modified cyclo(*L*-Lys-*L*-Lys). a) EDCI/HOBt/DMSO/CH_2Cl_2; b) piperidine/DMF/60 °C; c) TFA/TIS/CH_2Cl_2; d) I_2/MeOH; e) DTT/N_2.

2 Experimental

2.1 Materials and characterizations

Boc-Lys(Cbz)-OH and Fmoc-Cys(Trt)-OH were purchased from Beijing Redwood Fine Chemical Co., Ltd. (China). All other reagents (available from VAS Chemical Reagent Company, Tianjin, China) were analytical grade and used without further purification unless otherwise noted.

Fourier transform infrared spectroscopy (FT-IR): the FT-IR spectra were recorded on a Prestige-21 (Shimadzu, Japan) IR Spectrometer. The IR spectra of gelators in solid and organogel state were recorded using the KBr disk technique, and scanned between the wavelengths of 4000 and 400 cm^{-1}.

Fluorescence spectroscopy: the fluorescence emission spectra of supramolecular organogels and the solution of the peptidomimetics were recorded on a Cary Eclipse spectrometer (Varian, USA) with excitation at 265 nm and emission data ranging between 250 and 600 nm.

Transmission electron microscopy (TEM): TEM images were taken on a JEM 1200EX (JEOL, Japan) microscope at 120 kV voltages. A drop of dilute solution of the gel-phase material of the corresponding gel was placed on carbon coated copper grids (300 mesh) and dried by slow evaporation for two days.

Field emission scanning electron microscopy (FE-SEM): FE-SEM images were obtained from an S-4800 FE-SEM (Hitachi, Japan). The gel samples were prepared by the supercritical drying method and then coated with gold for 90 s at 5 kV voltages on silicon slices.

Oscillatory rheology: rheological measurements were performed on a strain-controlled MCR301 rheometer (Anton-Paar, Austria) using the parallel plate geometry at 25 °C. The storage and loss moduli were measured with a frequency sweep test (0.1–100 Hz).

NMR experiment: ^{1}H and ^{13}C NMR measurements were carried out on an Advance DRX 500 Bruker A&T Center BNU Instrument (Bruker, Germany) operating at 500 MHz. All spectra were recorded in DMSO-d_6.

Mass spectrometry: mass spectra were recorded on a G2 QTOF high-resolution mass spectrometer (Waters, USA).

Melting point tests: the melting points (m.p.) were obtained on a XT5B melting point apparatus (TianGuang, China) and uncorrected.

Circular dichroism (CD): CD was collected on a Jasco J-810 CD Spectro-meter (Jasco, Japan). CD spectra were measured over the range of 180–350 nm. The optical chamber was continually flushed with nitrogen.

Wide angle X-ray diffraction measurements: the organogels were freeze-dried to give rise to xerogels. XRD patterns were measured from xerogel by Ultima IV Instrument (Rigaku, Japan) using Cu Kα (λ=1.5405 Å) radiation.

Gelation tests: a weighed amount of potential gelator and the organic solvent were added into a sealed glass vial to make a total of 1 g of the mixture and heated to get a clear solution. The solution was then cooled back to room temperature in the air. The gelation (G) was confirmed by inverting the glass vial and the solution inside was no evident to flow. Systems in which only solution remained until the end of the tests were referred to as soluble (S).

2.2 Synthesis of Fmoc-Cys(Trt)-DKP-Lys-Fmoc-Cys-(Trt) (3)

To a solution of Fmoc-Cys(Trt)-OH (17.58 g, 30 mmol) in CH_2Cl_2 (200 mL) was added EDCI (7.67 g, 40 mmol) and TEA (2 mL) followed by the addition of HOB*t* (5.43 g, 40 mmol). The reaction mixture was stirred for 2 h at 0 °C and then added dropwise a solution of DKP-Lys·2HBr (**1**) (4.18 g, 10 mmol) in DMSO (30 mL). Upon completion of the addition, the reaction mixture was stirred at r.t. for 48 h and subsequently washed with saturated NaCl solution (3×100 mL), dried over Na_2SO_4, filtered, concentrated, and finally purified by chromatography on silica gel (EA/MeOH =10:1) to give rise to **3** as a white solid with a yield of 60%. m.p.: 125–128 °C. $[\alpha]_D^{20}$ (DMSO, *C*=0.1)=–30.03. IR (film) 3262 (ν_{N-H}), 1676 (amide I), 1564 (amide II) cm^{-1}. ^{1}H NMR (500 MHz, DMSO-d_6) δ 8.11–8.06 (m, 1H), 7.88 (d, *J*=5.2 Hz, 2H), 7.84 (t, *J*=3.6 Hz, 1H), 7.74 (d, *J*=5.2 Hz, 2H),7.62 (d, *J*=8.4 Hz, 1H),7.40 (td, *J*=7.5, 2.4 Hz, 2H), 7.35–7.27 (m, 13H), 7.27–7.22 (m, 4H), 4.34–4.28 (m, 1H), 4.25–4.17 (m, 2H), 4.06–3.99 (m, 1H), 3.73 (m, 1H), 3.05–2.91 (m, 2H), 2.43–2.31 (m, 2H), 1.71–1.53 (m, 2H), 1.37–1.23 (m, 4H) ppm. ^{13}C NMR (125 MHz, DMSO-d_6) δ 170.0, 168.4, 155.8, 144.8, 143.78, 140.9, 129.6, 128.5, 128.1, 127.5, 127.2, 125.9, 120.6, 66.3, 60.2, 54.2, 47.1, 34.6, 33.2, 29.1, 22.3, 21.2, 14.5 ppm. HRMS Calcd. for $C_{86}H_{82}O_8N_6S_2$: 1390.5636; found: 1391.5792 ([M+H]$^+$), 1414.5657 ([M+Na]$^+$). Anal. Calcd. for $C_{86}H_{82}O_8N_6S_2$: C 74.22, H 5.94, N 6.04, S 4.61; found C 74.44, H 5.93, N 5.88, S 4.54.

2.3 Synthesis of Cys(Trt)-DKP-Lys-Cys(Trt) (4)

A 0.5 g **3** (0.36 mmol) was dissolved in 10 mL co-solvent of piperidine/DMF (*v*/*v*=1:4) and stirred at 60 °C for 3 h. The reaction mixture gradually turned turbid. It was then precipitated into 300 mL diethyl ether and washed with 100 mL diethyl ether 3 times. The precipitates were gathered by filtration and purified by chromatography on silica gel ($CHCl_3$/MeOH=9:1) to give rise to **4** as a white solid with a yield of 70%. m.p.: 105–107 °C; $[\alpha]_D^{20}$ (DMSO, *C*=0.1)= –28.30. IR (film) 3311 (ν_{N-H}), 1666 (amide I), 1520 (amide II) cm^{-1}. ^{1}H NMR (500 MHz, DMSO-d_6) δ 8.12 (s, 1H), 7.81 (s, 1H), 7.36–7.16 (m, 15H), 3.75 (s, 1H), 3.08 (t, *J*=6.4 Hz, 1H), 2.94 (d, *J*=46.6 Hz, 2H), 2.34 (dd, *J*=11.5, 5.5 Hz, 1H), 2.18 (dd, *J*=11.2, 7.6 Hz, 1H), 1.71–1.54 (m, 2H), 1.39–1.25 (m, 4H) ppm. ^{13}C NMR (125 MHz, DMSO-d_6) δ 173.3, 168.4, 145.0, 129.6, 128.5, 127.1, 66.0, 54.5, 54.4, 38.8, 37.8, 33.2, 29.00, 22.2 ppm. HRMS Calcd. for $C_{56}H_{62}O_4N_6S_2$: 946.4274; found: 947.4346 ([M+H]$^+$), 969.4171 ([M+Na]$^+$). Anal. Calcd. for $C_{56}H_{62}O_4N_6S_2$: C 71.00, H 6.60, N 8.87, S 6.77; found C 71.02, H 6.66, N 8.92, S 6.47.

2.4 Synthesis of Fmoc-Cys-DKP-Lys-Fmoc-Cys (5)

To a solution of 1 g **3** (0.72 mmol) in CH_2Cl_2 (6 mL) was added triisopropylsilane (4 mL) followed by TFA (4 mL). The reaction mixture was stirred for 30 min at r.t. during which the bright orange solution turned colourless. The mixture was concentrated under reduced pressure. The residue was suspended in diethyl ether, centrifuged, the supernatant was discarded and the pellets were resuspended in diethyl ether with 5 times. Finally the pellets were dried

under reduced pressure to give rise to **5** as a white solid with a yield of 90 %. m.p.: 150–153 °C; $[\alpha]_D^{20}$(DMSO, *C*=0.1)= −34.34. IR (film) 3297 (ν_{N-H}), 1677 (amide I), 1539 (amide II), 2565 (–SH) cm^{-1}. ^1H NMR (500 MHz, DMSO-d_6) δ 8.12 (s, 1H), 8.01 (s, 1H), 7.90 (d, *J*=7.4 Hz, 2H),7.74 (d, *J*=4.1 Hz, 2H), 7.58 (d, *J*=8.1 Hz, 1H), 7.42 (t, *J*=7.3 Hz, 2H), 7.33 (t, *J*=7.1 Hz, 2H), 4.34–4.29 (m, 1H), 4.25 (dd, *J*=18.7, 6.9 Hz, 2H), 4.06 (d, *J*=5.2 Hz, 1H), 3.78 (s, 1H), 3.05 (dd, *J*=18.9, 5.8 Hz, 3H), 2.84–2.60 (m, 2H), 2.41–2.16 (m, 1H), 1.66 (d, *J*=33.6 Hz, 2H), 1.40–1.28 (m, 4H) ppm. ^{13}C NMR (125 MHz, DMSO-d_6) δ 170.1, 168.4, 156.4, 144.1, 140.6, 128.1, 127.5, 125.8, 120.6, 66.1, 60.3, 57.8, 54.4, 47.1, 33.2, 29.2, 26.8, 22.3 ppm. HRMS Calcd. for $C_{48}H_{54}O_8N_6S_2$: 906.3445; found: 929.3487 ($[M+Na]^+$). Anal. Calcd. for $C_{48}H_{54}O_8N_6S_2$: C 63.56; H 6.00; N 9.26; S 7.07; found C 63.48, H 5.82, N 8.99, S 7.10.

2.5 Synthesis of Cyclo(Fmoc-Cys-DKP-Lys-Fmoc-Cys) (6)

To a solution of 1 g **3** (0.72 mmol) in 500 mL MeOH was added dropwise a solution of 0.5 g I_2 in 200 mL MeOH. The reaction mixture was stirred for 12 h at r.t. The solution was concentrated in vacuum to about 20 mL and diluted with 200 mL CH_2Cl_2, washed with 1% $Na_2S_2O_3$, in which the bright orange solution turned colourless. The washed organic solution was dried over anhydrous Na_2SO_4 and evaporated in vacuum. A buff solid was obtained with a yield of 55 %. m.p.: 146–148 °C; $[\alpha]_D^{20}$ (DMSO, *C*=0.1)=–8.01. IR (film): 3305 (ν_{N-H}), 1665 (amide I), 1530 (amide II). ^1H NMR (DMSO-d_6): δ 8.10–7.80 (m, 4H), 7.80–7.55 (m, 3H), 7.34 (m, 4H), 4.37–4.17 (m, 4H), 3.89 (d, *J*=16.3 Hz, 1H), 3.40–3.24 (m, 2H), 3.10–2.90 (m, 2H), 1.81–1.54 (m, 2H), 1.49–1.20 (m, 4H) ppm. ^{13}C NMR (DMSO-d_6): δ 170.4, 168.1, 156.3, 144.3, 141.2, 128.1, 127.6, 125.8, 120.6, 66.2, 54.2, 54.1, 47.1, 40.9, 32.3, 28.8, 21.0, 20.6 ppm. HRMS Calcd. for $C_{48}H_{52}N_6O_8S_2$: 904.3288; found: 905.3371 ($[M+H]^+$). Anal Calcd. for $C_{48}H_{52}N_6O_8S_2$: C 63.70; H 5.79; N 9.29; S 7.09; found C 63.63; H 5.29; N 9.55; S 7.51.

2.6 Synthesis of Cyclo(Cys-DKP-Lys-Cys) (7)

Route 1: 0.5 g **4** was dissolved in 500 mL MeOH and then to it a solution of 1 g I_2 in 200 mL MeOH was dropwise added. The reaction mixture was stirred for 12 h at r.t. Then the solution was concentrated in vacuum to about 20 mL and diluted with 200 mL CH_2Cl_2, washed with 1% $Na_2S_2O_3$, in which the bright orange solution turned colourless. This washed organic solution was dried over anhydrous Na_2SO_4 and evaporated in vacuum. Beige solids were obtained with a yield of 70%.

Route 2: 0.5 g **6** was dissolved in 15 mL co-solvent of piperidine/DMF (*v*/*v*=1:4) and stirred at 60 °C for 3 h. The reaction mixture gradually turned turbid. It was then precipitated into 200 mL diethyl ether and washed with 100 mL diethyl ether 3 times. The precipitate was gathered by filtration, and evaporated in vacuum. Beige solids were obtained with a yield of 75%. m.p.: 192–194 °C; $[\alpha]_D^{20}$ (DMSO, *C*=0.1)=−10.00. IR (film) 3295 (ν_{N-H}), 1673 (amide I), 1521 (amide II). ^1H NMR (400 MHz, DMSO-d_6) δ 8.62–8.49 (m, 1H), 8.17–8.11 (m, 1H), 7.32 (dd, *J*=26.4, 7.1 Hz, 2H), 4.02 (s, 1H), 3.81 (s, 1H), 3.24–2.96 (m, 4H), 1.67 (d, *J*=45.7 Hz, 2H), 1.41 (d, *J*=25.4 Hz, 4H) ppm. ^{13}C NMR (DMSO-d_6): δ 173.0, 167.7, 54.2, 44.1, 32.6, 28.8, 22.8, 21.9, 21.3 ppm. HRMS Calcd. for $C_{18}H_{32}N_6O_4S_2$: 460.1926; found: 461.2004 ($[M+H]^+$).

2.7 Synthesis of Cys-DKP-Lys-Cys (8)

A 0.3 g **7** was dissolved in 30 mL DMSO. To this mixture, a solution of 1,4-dithiothreitol (0.5 g in 2 mL MeOH) was added and the solution was stirred at 37 °C under a nitrogen atmosphere. After 5 h, the mixture was poured into H_2O (300 mL) and extracted with ethyl acetate (3×30 mL). The water layers were combined, and freeze dried to give a white solid with a yield of 65%. m.p.: 170–173 °C; $[\alpha]_D^{20}$ (DMSO, *C*=0.1)=−26.20; IR (film) 3305 (ν_{N-H}), 1665 (amide I), 1548 (amide II), 2550 (–SH) cm^{-1}. ^1H NMR (400 MHz, DMSO-d_6) δ 8.11 (s, 1H), 8.03 (s, 1H), 3.80 (s, 1H), 3.53 (s, 1H), 3.05 (d, *J*=12.2 Hz, 2H), 2.74 (s, 2H), 1.66 (s, 2H), 1.37 (d, *J*=35.7 Hz, 4H) ppm. ^{13}C NMR (DMSO-d_6): δ 173.0 168.3 56.9 54.4 33.4 30.0 29.3 27.5 22.3 ppm. HRMS Calcd. for $C_{18}H_{34}N_6O_4S_2$: 462.2083; found 463.2154 ($[M+H]^+$).

3 Results and discussion

3.1 Synthesis

The synthetic pathway of symmetrical peptidomimetics **3–8** is outlined in Scheme 1. The starting cyclo(*L*-Lys-*L*-Lys) (**1**) was first prepared according to literatures [22,23]. **3** was obtained from the coupling reaction of **1** and **2** in the presence of EDCI/HOBT. A co-solvent of piperidine/DMF was employed to deprotect Fmoc to give **4** retaining S-Trt. Thanks to the same distance of two pendent –SH groups located from the cyclic dipeptide core, the bicyclic pepetidomimetic **6** was easily prepared either from **3** by deprotecting Trt or from **5** by the oxidation of –SH into –SS– using I_2/MeOH. It provides a preparative route for bigger cyclic- and bicyclic peptidomimetics. Although this transformation would alter the π-π interactions of Fmoc groups in **5**, it provides a protocol to synthesize bicyclic peptidomimetics through the –SH to –SS– oxidation. Meanwhile, the noncyclic **5** was prepared from **3** by deprotecting Trt in TFA/TIS. Moreover, the bicyclic peptidomimetic **7** was created either from **4** in I_2/MeOH or **6** in a piperidine/DMF co-solvent. Finally, **7** was transformed into **8** through the DTT-induced –SS– into –SH reduction reaction under a

nitrogen atmosphere. However, **8** is unstable in the air because of the liable oxidation of –SH into –SS–. Besides **6** and **7**, no other polycyclic products were found in the preparation process of the symmetrical peptidomimetics in this study.

3.2 Gel performance

Currently, an investigation into the molecular design of LMWGs enabling to gelate water and/or organic solvents remains a great challenge [3,5]. In this context, Fmoc and Trt protected cysteine was selected to modify cyclic dipeptide **1**. As is well known, Fmoc was routinely incorporated to facilitate the self-assembly of a number of LMWGs in the gelation process [24,25]. However, Trt was seldom demonstrated to promote the gelation capability of LMWGs. After introducing Fmoc and Trt protected cysteine to **1**, the resulting peptidomimetics **3–8** exhibited the diverse gelation behavior as summarized in Table 1.

As can be seen, **3** and **4** with S-protected by Trt are insoluble in water, but soluble in most aliphatic and aromatic solvents showing no gelation ability. After the deprotection of Trt, both noncyclic **5** and bicyclic **6** became organogelators enabling to gelate most polar and chlorinated organic solvents. Moreover, ultrasound can boost **5** to form a weak organogel instead of precipitates during the cooling process in acetonitrile, but it cannot work for **6**. This is maybe due to Trt holding three phenyl rings with different orientations, while Fmoc having a flat conjugate structure making a great contribution to the π-π interactions [26]. So the protecting groups dominated the gelation performance of the peptidomimetics **3–8** in this study, in which a non-gelator with Trt can be transformed into an organogelator with Fmoc after the deprotection. In accordance with previous reports, Fmoc are indeed more advantageous over Trt to boost the self-assembly of LMWGs. Meanwhile, the minimum gelation concentration (MGC) of the gelator **6** was obviously increased after the oxidation of –SH in **5** into –SS–, most likely due to the formation of –SS– interfering with π-π stacking in the self-assembly of the gelator. Upon removing the hydrophobic Fmoc groups, however, both **7** and **8** became water-soluble showing no gelation.

3.3 Rheological measurements

The viscoelastic properties of the obtained organogels were investigated. The dynamic mechanical spectra of the **5** and **6** organogels at their MGC in 1,2-dichloroethane were tested at 25 °C, respectively. As can be seen in the insets of Figure 1, the elastic modulus (G') of both **5** and **6** presented a long plateau at a low strain range, and began to sharply decrease in a range of γ_0=0.5% to 50%. Therefore, γ_0 was restricted to 0.1% for the rheological testing. It was found that the G' was an order of magnitude higher than the G'' at all the testing frequencies, displaying an elastic rather than viscous material of both the **5** and **6** organogels. Moreover, the complex viscosity (η^*) was linearly depressed with the increasing of frequency without showing any Newtonian plateau, which was also observed in other organogel (Figure S1, Supporting Information online). This rheological behavior is characteristic of solid-like materials, and thus the samples can be qualified as true organogels [21,27].

Furthermore, as shown in Figure 1, both the G' and G'' of the **5** organogel are always higher than those of the **6** organogel in the range of testing frequencies as a whole. For example, at ω=1 and 100 Hz, the G' of the former reach 3.0×10^3 and 2.1×10^4 Pa, whereas those of the latter only attain 1.6×10^3 and 4.3×10^3 Pa, separately. Especially, the **5** organogel became more robust than the **6** organogel at higher frequencies. The results further revealed that **5** is stronger than **6** as an organogelator in most organic solvents probably due to the formation of –SS– breaking down the

Table 1 Results of gelation test and minimum gelation concentrations (MGC, wt%) of gelators in various organic solvents at r.t.

Solvents	**3**	**4**	**5**	**6**	**7**	**8**
Benzene	P [a)]	P	I [b)]	I	I	I
Tetrachloromethane	I	I	I	I	I	I
Toluene	S [c)]	P	PG [d)]	S(4)	I	I
o-Dichlorobenzene	S	S	G(0.3) [e)]	S	S	S
1,2-Dichloroethane	S	S	G(1)	G(1)	I	I
1,1,2,2-Tetrachloroethane	S	S	S	G(2.5)	I	I
CH_2Cl_2	S	S	G(1)	G(4)	I	I
$CHCl_3$	S	S	G(0.8)	G(4)	I	I
Tetrahydrofuran (THF)	S	S	G(3)	G(3)	I	I
1,4-Dioxane	S	S	G(2)	G(2.5)	I	I
DMF	S	S	S	S	S	S
DMSO	S	S	S	S	S	S
Acetonitrile	I	I	UG(2) [f)]	I	I	I
CH_3OH	P	S	I	I	I	S
H_2O	I	I	I	I	S	S

a) P: precipitation; b) I: insoluble upon heating; c) S: soluble (>5 wt%); d) PG: partial gelation; e) G: gelation; f) UG: gelation by ultrasound.

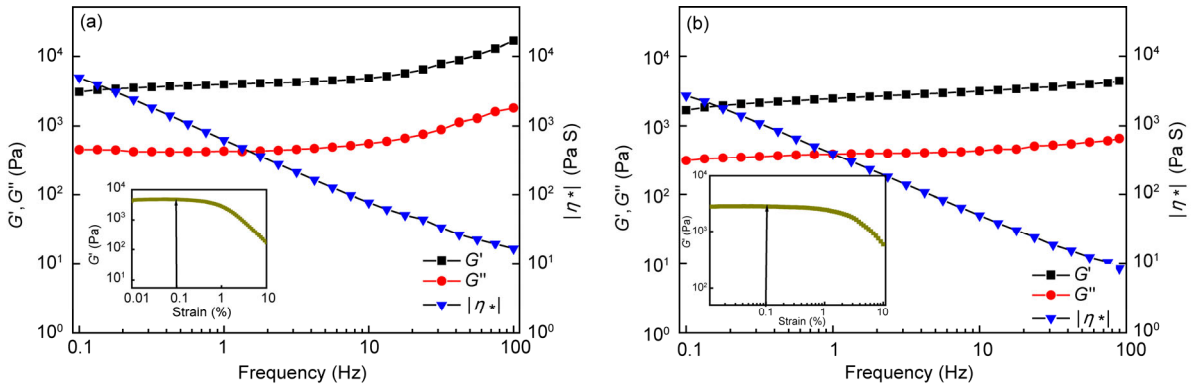

Figure 1 Viscoelastic behaviors of **5** (a) and **6** organogel (b) in 1,2-dichloroethane (1 wt%). Frequency sweep using a constant strain of 0.1% from 0.1 to 100 Hz at 25 °C.

π-π stacking interactions between Fmoc groups in the resulting peptidomimetic.

3.4 Morphology observations

The interior morphologies of the self-constructed **5** and **6** gels were analyzed by TEM and SEM observations. Entangled nanofiber 3D networks of organogels of **5** in 1,2-dichloroethane and *o*-dichlorobenzene and **6** in 1,2-dichloroethane and 1,1,2,2-tetrachloroethane are shown in Figure 2. A careful inspection of these images depicted in Figure 2(a–d) presented that the widths of the nanofibers are within a range of 10–20 nm, and short nanofibrils are mutual twisted to form dense clusters. Also as seen in Figure 2(e–h), a significant amount of assemblies that consist of tape-like aggregates were formed with an average width of 30 nm. For the organogel of **6** formed in 1,2-dichloroethane, these nano-tapes were extended into micrometer scale lengths and seemed to stack on top of each other at intersections to give rise to a meshed structure. However, for the organogel of **6** obtained in 1,1,2,2-tetrachloroethane, the well-shaped tape-like aggregates were visible with an average length of hundreds of nanometers. As a result, these nanofibrils and nanotapes both built up a 3D entangled network to absorb a vast amount of organic solvents to create physical organogels.

3.5 Determination of driving forces in self-assembly

Fluorescence spectroscopy is broadly used to investigate into the π-π interactions between the fluorenyl groups in the solution and gel phases [13,25,26,28–30]. As shown in Figures 3 and 4, a distinct single fluorescence peak was observed at ~314 nm for the gelator **5** and **6** at low concentrations (0.01 wt%–0.5 wt%, red lines) in different solvents. This peak is indicative of the Fmoc groups of resulting peptidomimetics in the monomeric state in the solution. As for the gelator **5**, this main florescence peak was red-shifted with the increasing of concentration in the tested solvents, indicating the beginning of excimer aggregation of fluorenes, for example, the formation of excited dimmers [31]. As the red shift of emission spectra of fluorene-type moieties in a parallel manner is somewhat larger than their antiparallel analogues [32,33], a small peak at ~360 nm in the organogels could be ascribed to that a small amount of the

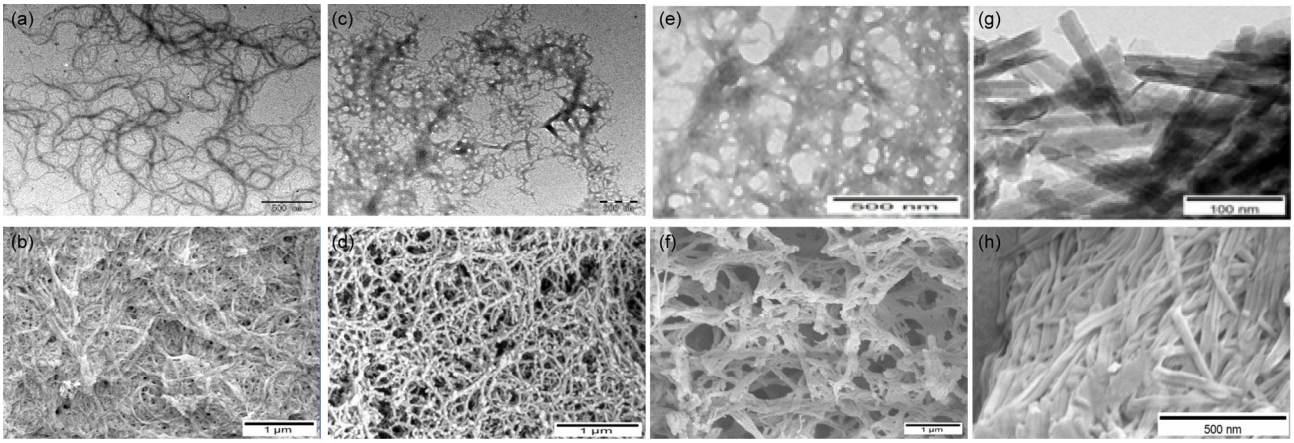

Figure 2 TEM and FE-SEM images of organogels. (a, b) **5** organogel in 1,2-dichloroethane; (c, d) **5** organogel in *o*-dichlorobenzene; (e, f) **6** organogel in 1,2-dichloroethane; (g, h) **6** organogel in 1,1,2,2-tetrachloroethane.

fluorenes overlap in a parallel fashion [25,33]. For the gelator **6** in the tested solvents, however, only a smaller red shift at ~321 nm was observed and the peak at 360 nm was not found, suggesting that the antiparallel stacking is favored in its fluorene overlapping.

Since the excimer peaks for the gelator **5** were red-shifted to the same extent at all tested solvents (Figure 3(a, b)), while the gelator **6** expressed only small red shifts, **5** was suggested to hold the more efficient overlapping of the aromatic moieties and stronger π-π interactions between fluorenyl groups. As the concentration of **5** was increased to its MGC value, a number of peaks appeared at 420–485 nm in its emission spectroscopy indicative of more than two of fluorenyl rings stacked efficiently in the gels via the π-π interactions [29,30,32]. The occurrence of these peaks implied that the extended self-assembled structures are formed in the organogels benefited from the π-π interactions. Noticeably, a broad peak with a maximum at about 460 nm appeared in the emission spectroscopy of the **6** organogel, possibly due to the presence of an extensive *J*-aggregate with fluorenyl rings [27]. The existence of this broad peak with particularly intense clearly illustrated that these Fmoc groups are located in highly hydrophobic environments and buried deeper in the self-assembled structures in the formed nanotapes [33]. This inference is also consistent with the model proposed for the self-assembly of **6** as shown in Figure 5. As a consequence, the π-π interactions between the fluorenyl groups provide part of the linkages in the extended chain structures.

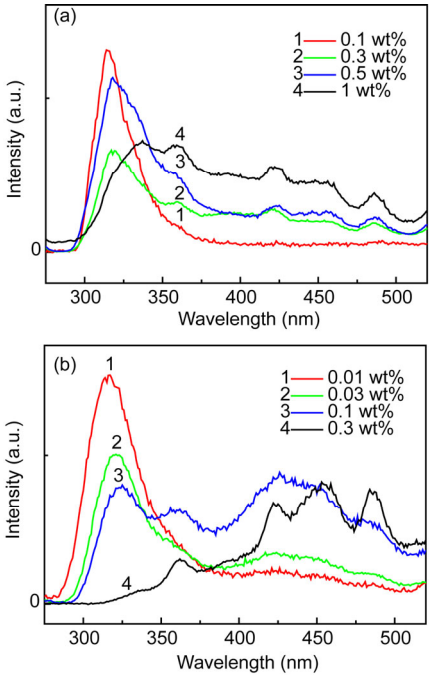

Figure 3 Fluorescence emission spectra of organogel of **5** in 1,2-dichloroethane (a) and in *o*-dichlorobenzene (b) ($\lambda_{excitation}$=265 nm).

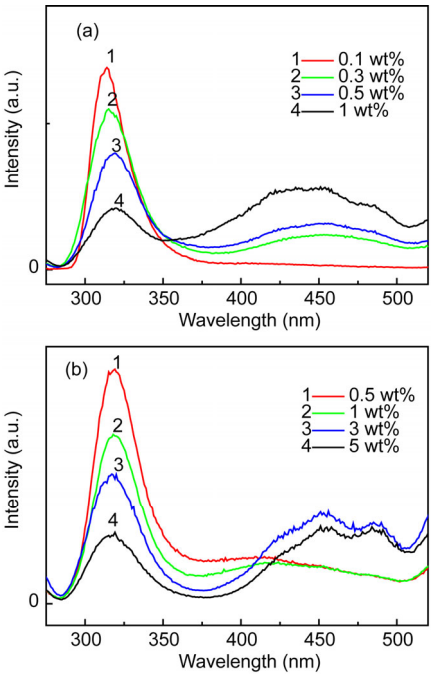

Figure 4 Fluorescence emission spectra of organogel of **6** in 1,2-dichloroethane (a) and in 1,1,2,2-tetrachloroethane (b) ($\lambda_{excitation}$=265 nm).

FT-IR spectroscopy is widely employed to shed light on the hydrogen bonds between the gelators in the gel state [5,29,30]. In Figure 6(a, b), the ν_{N-H} signals of both **5** and **6** in DMSO solution appeared at 3461 cm^{-1}, and amide I and amide II band at 1678 and 1540 cm^{-1}, clearly indicating non-hydrogen-bond occurrence in them. As the amide I band is very sensitive to secondary structure [13], the **5** gelator displayed double peaks for amide I, one blue-shift and another red-shift as compared with the single amide I band as seen in DMSO. The obvious peak centered at around 1648 cm^{-1} probably pointed to the presence of disordered structures [33], although another signal at about 1685 cm^{-1} was possibly assigned to hydrogen-bonded β-sheet structure, and most likely existed in an antiparallel configuration [13,25,34,35]. This is due to the fact that the molecular sequence of **5** being flexible, steric, and/or other

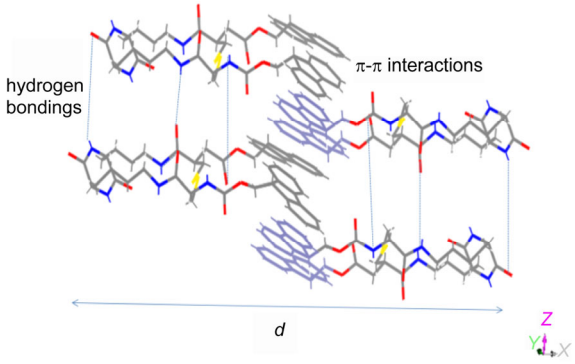

Figure 5 Schematic description of possible self-assembled microstructure of organogel **6**.

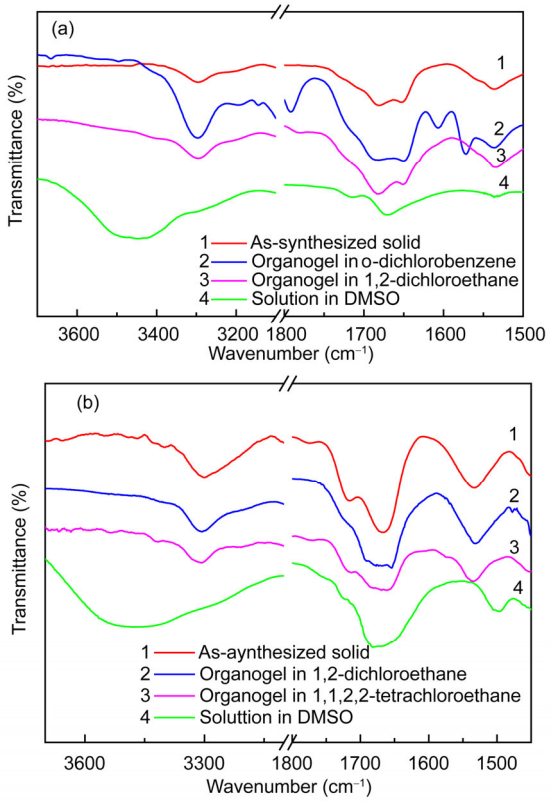

Figure 6 FT-IR spectra of **5** (a) and **6** (b) in solution, gel and solid states.

constraints resulted in this disordered secondary structure [35]. The shifting of ν_{N-H} to ~3297 cm^{-1} and amide II band to ~1543 cm^{-1} further demonstrated the formation of hydrogen bonds of **5** in the gel and solid states. Unlike the **5** gelator, there are individualized broad peaks in the region of 1660–1685 cm^{-1} for the **6** gelator, maybe stemmed from reverse β-turns [5,36]. This assertion was also supported by the following CD analysis. Meanwhile, it also gave peaks at ~3310 for the N–H stretching vibration and 1554 cm^{-1} for amide II band, in which the characteristic shifts for hydrogen-bonded were seen, but the relatively smaller red-shifts were suggested a relatively poor hydrogen-bonding environment than in the **5** organogel.

As described above, the π-π interactions and hydrogen bonds are indeed the major driving forces for the gelation of the peptidomimetics. Taking account of FT-IR results of **5** with the disordered secondary structure and **6** in the β-turn formation, the CD spectrum and X-ray diffraction (XRD) analyses of the **6** organogel were also conducted in this study.

It is well documented that each β-turn consists of four amino acid residues (labelled *i*, *i*+1, *i*+2 and *i*+3), and has possession of an inter-main-chain hydrogen bond between the C=O of residue *i* and the N–H of residue *i*+3 [37,38]. The **6** gelator was endowed with –SS– between residue *i* and *i*+3, which made the two residues closer, and consequently made it easier to form hydrogen bond between them. As shown in Figure 7, the CD spectrum of the **6** organogel obtained in 1,1,2,2-tetrachloroethane depicted a positive peak at 205 nm and negative peaks at 180–190 and 220–230 nm characteristic of the β-turns conformation of a polypeptide [5]. Besides, a negative broad band at near 240–270 nm was also observed for the π-π transition of terminal aromatic moiety [32], and then the positive peaks at 270–320 nm mainly due to the fluorenyl groups were deemed to be stacked in a helical orientation as often seen in other Fmoc-peptide gel systems [26,28,35]. As a result, the gelator **6** is inclined to self-assemble by the β-turn formation, and the surmise is in agreement with FTIR results, and is demonstrated by CD study.

To further understand the molecular arrangements and the orientation of the gelator molecules in the gel state, the dried organogels of **5** and **6** were measured by using XRD equipment. The xerogels obtained from their organogels by a freezing method created the sponge-like configuration, instead of the typical crystal. The xerogel formed with **5** in 1,2-dichloroethane showed no good diffraction peaks, which corresponded to its FT-IR result with the disordered secondary structure. However, the xerogel **6** obtained in 1,2-dichloroethane presented specific XRD pattern as outlined in Figure 8. This diffraction pattern exhibited four periodical reflections at 1.83, 0.92, 0.61 and 0.46 nm, which are almost exactly in the ratio 1:1/2:1/3:1/4. It implied the

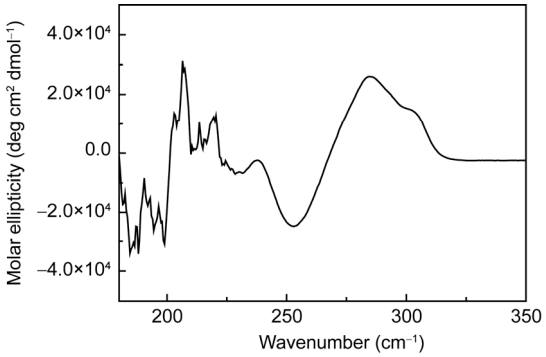

Figure 7 CD spectrum of **6** organogel in 1,1,2,2-tetrachloroethane.

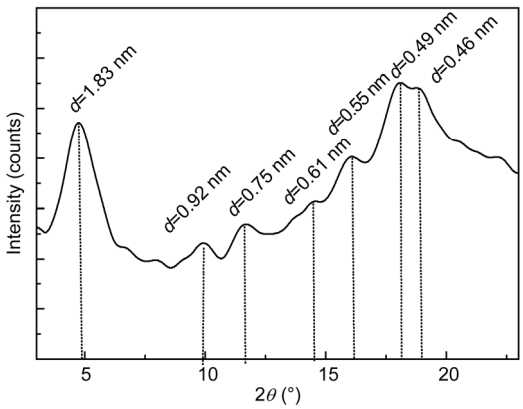

Figure 8 XRD pattern of organogel of **6** in 1,2-dichloroethane.

xerogel holding a lamellar organization [17,39]. The XRD pattern of the xerogel **6** formed in 1,1,2,2-tetrachloroethane also depicted periodical reflections (Figure S2) and the long spacing (*d*) value is 1.72 nm. However, the long *d* spacing of these aggregates is smaller than twice the fully extended molecular length of one **6** molecule**,** but larger than the length of one molecule (1.391 nm, calculated by MM2, minimize energy method, Chem. Office 3D). The results indicated that the organogel **6** is constructed by an interdigitated bilayered structure [31,40], wherein the molecules are connected by the intra- and interlayer hydrogen bonds and π-π interactions. The proposed interdigitated bilayer structure is represented in Figure 5.

The self-assembly of the gelator **6** in organic solvents leading to organogels is a hierarchical process as shown in Figure S3. In solution, **6** is in the free state of single molecule. When a thermal stimulus is provided, **6** should adopt the β-turn secondary structures by the π-π stacking and hydrogen bonds to form an amphiphilic structure that the aromatic groups cluster on the one side of molecules. The regular β-turn structures are parallel bilayer stacked along their long axis to form flat single nanofiber. Elongation and arrangement of the nanofibers in 3D space lead to longer and thicker tapes, which are further self-assembled to a fibrillar network. The resulting 3D scaffolds can entrap a large amount of organic solvents and afford a self-supporting organogel. However, these non-covalent interactions in the network can be disrupted by heating, and the gel can be returned to the soluble state. This course enables the resulting gels to be recycled and reversible.

4 Conclusions

In summary, a series of symmetrical peptidomimetics **3–8** were synthesized and characterized by means of ^{1}H and ^{13}C NMR, MS, IR and elemental analyses. The peptidomimetics **3** and **4** with Trt exhibited high solubility in most organic solvents. Both non-cyclic peptidomimetic **5** and bicyclic peptidomimetic **6** with Fmoc possessed a capability to gel a number of organic solvents forming thermo-reversible gels with self-assembled fibrillar 3D networks as well as diverse secondary structures due to the tiny structural modifications. Meanwhile, XRD studies suggested the existence of interdigitated bilayers in the xerogel obtained from **6** in 1,2-dichloroethane. Its β-turn secondary structure was supported by FT-IR and CD measurements. The findings clearly indicated that 2,5-DKP core is a commendatory structural unit in the design and synthesis of LMWGs, wherein Fmoc is favorable to boost the self-assembly of LMWGs over Trt, and the redox reaction of thiol into disulfide also plays an important role in tuning their gelation behavior. With the current interest in these unique molecules and their organogels, it is reasonably anticipated that further exciting developments and practical uses of 2,5-DKP derivatives will occur sooner.

Acknowledgments This work was supported by the National Natural Science Foundation of China (21174018).

Conflict of interest The authors declare that they have no conflict of interest.

Supporting information The supporting information is available online at http://chem.scichina.com and http://link.springer.com/journal/11426. The supporting materials are published as submitted, without typesetting or editing. The responsibility for scientific accuracy and content remains entirely with the authors.

1 Hanabusa K, Suzuki M. *Polym J*, 2014, 46: 776–782
2 Buerkle LE, Rowan SJ. *Chem Soc Rev*, 2012, 41: 6089–6103
3 Adams DJ. *Macrom Biosci*, 2011, 11: 160–173
4 Xie ZG, Zhang AY, Ye L, Feng ZG. *Soft Matter*, 2009, 5: 1474–1482
5 Kar T, Debnath S, Das D, Shome A, Das PK. *Langmuir*, 2009, 25: 8639–8648
6 Dasgupta A, Mondal JH, Das D. *RSC Adv*, 2013, 3: 9117–9149
7 Zhang SG, Marini DM, Hwang W, Santoso S. *Curr Opin Chem Biol*, 2002, 6: 865–871
8 Koutsopoulos S, Unsworth LD, Nagai Y, Zhang SG. *Proc Natl Acad Sci USA*, 2009, 106: 4623–4628
9 Zhang YL, Yang B, Xu LX, Zhang XY, Tao L, Wei Y. *Acta Chim Sinica*, 2013, 71: 485–492
10 Chen J, Wu W, McNeil AJ. *Chem Commun*, 2012, 48: 7310–7312
11 Frederix PW, Scott GG, Abul-Haija YM, Kalafatovic D, Pappas CG, Javid N, Hunt NT, Ulijn RV, Tuttle T. *Nat Chem*, 2015, 7: 30–37
12 Gazit E. *Nat Chem*, 2015, 7: 14–15
13 Cheng G, Castelletto V, Moulton CM, Newby GE, Hamley IW. *Langmuir*, 2010, 26: 4990–4998
14 Manchineella S, Govindaraju T. *RSC Adv*, 2012, 2: 5539–5542
15 Mash EA. *Cryst Eng Comm*, 2014, 16: 8620–8637
16 Borthwick AD. *Chem Rev*, 2012, 112: 3641–3716
17 Hanabusa K, Matsumoto M, Kimura M, Kakehi A, Shirai H. *J Colloid Interf Sci*, 2000, 224: 231–244
18 Delatouche R, Durini M, Civera M, Belvisi L, Piarulli U. *Tetrahedron Lett*, 2010, 51: 4278–4280
19 Hoshizawa H, Minemura Y, Yoshikawa K, Suzuki M, Hanabusa K. *Langmuir*, 2013, 29: 14666–14673
20 Sasaki Y, Akustu Y, Matsui M, Suzuki K, Sakurada S, Sato T, Kisara K. *Chem Pharm Bull*, 1982, 30: 4435–4442
21 Xie ZG, Zhang AY, Ye L, Wang X, Feng ZG. *J Mater Chem*, 2009, 19: 6100–6102
22 a) Majó MA, Bou JJ, Herranz C, Muñoz-Guerra S. *Macromol Chem Phys*, 2006, 207: 615–620; b) Zong QY, Geng HM, Zhang AY, Ye L, Wang X, Feng ZG. *Acta Chim Sinica*, 2015, 73: 423–430
23 a) Kaur N, Zhou B, Breitbeil F, Hardy K, Kraft KS, Trantcheva I, Phanstiel O IV. *Mol Pharm*, 2007, 5: 294–315; b) Geng HM, Zong QY, Zhang AY, Ye L, Wang X, Feng ZG. *Chin J Appl Chem*, 2015, 32: 900–908
24 Fleming S, Ulijn RV. *Chem Soc Rev*, 2014, 43: 8150–8177
25 Yang ZM, Gu HW, Fu DG, Gao P, Lam GK, Xu B. *Adv Mater*, 2004, 16: 1440–1444
26 Shao H, Parquette JR. *Chem Commun*, 2010, 46: 4285–4287
27 Smith AM, Williams RJ, Tang C, Coppo P, Collins RF, Turner ML, Saiani A, Ulijn RV. *Adv Mater*, 2008, 20: 37–41
28 Nguyen MM, Eckes KM, Suggs LJ. *Soft Matter*, 2014, 10: 2693–2702
29 Xie ZG, Zhang AY, Ye L, Feng ZG. *Acta Chim Sinica*, 2008, 23: 2620–2624

30 Dou X, Li P, Zhang D, Feng CL. *Soft Matter*, 2012, 8: 3231–3238
31 Tang C, Ulijn RV, Saiani A. *Langmuir*, 2011, 27: 14438–14449
32 a) Xu XD, Chen CS, Lu B, Cheng SX, Zhang XZ, Zhuo RX. *J Phys Chem B*, 2010, 114: 2365–2372; b) Schweitzer D, Hausser KH, Haenel MW. *Chem Phys*, 1978, 29: 181–185
33 a) Wang HM, Yang CH, Tan M, Wang L, Kong DL, Yang ZM. *Soft Matter*, 2011, 7: 3897–3905; b) Gosal WS, Clark AH, Pudney PDA, Ross-Murphy SB. *Langmuir*, 2002, 18: 7174–7781; c) Gosal WS, Clark AH, Pudney PDA, Ross-Murphy SB. *Biomacromolecules*, 2004, 5: 2408–2419
34 Zhu P, Yan X, Su Y, Yang Y, Li J. *Chem Eur J*, 2010, 16: 3176–3183
35 a) Nalluri SK, Shivarova N, Kanibolotsky AL, Zelzer M, Gupta S, Frederix PW, Skabara PJ, Gleskova H, Ulijn RV. *Langmuir*, 2014, 30: 12429–12437; b) Tang C, Smith AM, Collins RF. *Langmuir*, 2009, 25: 9447– 9453
36 Dave N, Troullier A, Mus-Veteau I, Duňach M, Leblanc G, Padrõs E. *Biophys J*, 2008, 78: 747–755
37 Koch O. *Mol Inf*, 2012, 31: 624–630
38 Gunasekaran K, Gomathi L, Ramakrishnan C, Chandrasekhar J, Balaram P. *J Mol Biol*, 1998, 284: 1505–1516
39 Tena-Solsona M, Miravet JF, Escuder B. *Chem Eur J*, 2014, 20: 1023–1031
40 John G, Masuda M, Yoshida K, Shinkai S, Shimizu T. *Langmuir*, 2001, 17: 7229–7232